The *ACA4* Gene of Arabidopsis Encodes a Vacuolar Membrane Calcium Pump That Improves Salt Tolerance in Yeast[1]

Markus Geisler[2], Nathalie Frangne, Eric Gomès, Enrico Martinoia, and Michael G. Palmgren*

Department of Plant Biology, The Royal Veterinary and Agricultural University, Thorvaldsensvej 40, DK–1871 Frederiksberg C, Denmark (M.G., E.G., M.G.P.); and Institut de Botanique, Physiologie Végétale, Université de Neuchâtel, 2007 Neuchatel, Switzerland (N.F., E.M.)

Several lines of evidence suggest that regulation of intracellular Ca^{2+} levels is crucial for adaptation of plants to environmental stress. We have cloned and characterized Arabidopsis auto-inhibited Ca^{2+}-ATPase, isoform 4 (ACA4), a calmodulin-regulated Ca^{2+}-ATPase. Confocal laser scanning data of a green fluorescent protein-tagged version of ACA4 as well as western-blot analysis of microsomal fractions obtained from two-phase partitioning and Suc density gradient centrifugation suggest that ACA4 is localized to small vacuoles. The N terminus of ACA4 contains an auto-inhibitory domain with a binding site for calmodulin as demonstrated through calmodulin-binding studies and complementation experiments using the calcium transport yeast mutant K616. ACA4 and PMC1, the yeast vacuolar Ca^{2+}-ATPase, conferred protection against osmotic stress such as high NaCl, KCl, and mannitol when expressed in the K616 strain. An N-terminally modified form of ACA4 specifically conferred increased NaCl tolerance, whereas full-length ATPase had less effect.

In plant cells, calcium functions as a second messenger coupling a wide range of extracellular stimuli to intracellular responses (Trewavas and Malho, 1998; Sanders et al., 1999). Recent evidence suggests that plants, like animals, produce graded responses resulting in Ca^{2+} "signatures" such as oscillations and waves of changing concentration (Ehrhardt et al., 1996; Jaffe and Creton, 1998; McAinsh and Hetherington, 1998). Plants are able to adjust to stresses, such as high-salt environments, by activating a signal transduction system involving calcium (Bressan et al., 1998; Epstein 1998; Serrano et al., 1999). NaCl causes a rapid increase in cytosolic calcium, although it is still unclear whether this increase mediates salt adaptation or acts as a general stress signal (Niu et al., 1995). An increase in external calcium ameliorates the inhibitory effect of salt (Niu et al., 1995; Wu et al., 1996). Insight into the underlying mechanism has been provided by the recent reports from Zhu and coworkers (Liu and Zhu, 1997, 1998; Zhu et al., 1998; Halfter et al., 2000). An Arabidopsis *sos3* mutant was identified that is hypersensitive to NaCl and LiCl, but whose phenotype is suppressed by millimolar levels of calcium (Zhu et al., 1998). *SOS3* encodes a protein that shares significant sequence similarity with the calcineurin B subunit from yeast and neuronal calcium sensors from animals (Liu and Zhu, 1998) and is involved in regulation of the SOS2 protein kinase (Halfter et al., 2000). Therefore, it seems likely that intracellular calcium signaling through a calcineurin-like pathway mediates the calcium effect on salt tolerance. This idea is in line with a report that activated yeast calcineurin facilitated salt-stress adaptation of transgenic plants (Pardo et al., 1998).

The plant vacuole contains millimolar [Ca^{2+}] and is thought to represent the major calcium store in plants (Bush, 1995; Muir and Sanders, 1997). In the vacuolar membrane, voltage-gated Ca^{2+}-release channels, as well as inositol 1,4,5-trisphosphate and cADP-Rib-sensitive calcium-release pathways have been identified as part of the system producing calcium signatures (Allen et al., 1995). The signaling machinery downstream of calcium is unknown; however, both calcium-activated phosphatases/kinases and calmodulin (CaM) isoforms (McAinsh et al., 1997) or CaM-like Ca^{2+}-binding proteins (Jang et al., 1998; Snedden and Fromm, 1998) are good candidates to function in decoding calcium specificity (McAinsh and Hetherington, 1998).

Low cytoplasmic calcium levels are achieved by the function of high-affinity primary Ca^{2+}-ATPases of the P-type and low-affinity H^+/Ca^{2+} antiporters (Evans and Williams, 1998; Geisler et al., 2000). It is possible that the increase in cytosolic calcium that follows NaCl exposure might be followed by an increased capacity of calcium pumps to down-regulate cytoplasmic calcium (Niu et al., 1995). Transcripts of plant endoplasmic reticulum (ER)

[1] This work was supported in part by the European Union Biotechnology program, the Danish Biotech III program, and the Alexander von Humboldt Foundation (Feodor-Lynen Fellowship to M.G.).

[2] Present address: Institut de Botanique, Physiologie Végétale, Université de Neuchâtel, 2007 Neuchâtel, Switzerland.

* Corresponding author; e-mail palmgren@biobase.dk; fax 45–3528–3333.

Ca^{2+}-ATPases also have been shown to accumulate upon NaCl treatment in tomato (*Lycopersicon esculentum*; Wimmers et al., 1992) and tobacco (*Nicotiana tabacum*; Perez-Prat et al., 1992). With this background, we aimed to clone and functionally characterize the Arabidopsis homologue (ACA4) of the cauliflower (*Brassica oleracea*) vacuolar membrane Ca^{2+}-ATPase BCA1 (Malmström et al., 1997). We show that ACA4 is situated in vacuoles and is a CaM-regulated Ca^{2+}-ATPase having an N-terminal regulatory domain. We also provide genetic evidence that ACA4 might be involved in calcium signaling upon treatment with salt.

RESULTS

Primary Structure of ACA4

To clone a Ca^{2+}-ATPase from vacuolar membranes of Arabidopsis, we aimed at cloning the Arabidopsis homologue of BCA1 (Malmström et al., 1997), a vacuolar membrane type IIB Ca^{2+}-ATPase from cauliflower (Askerlund, 1997). We employed a method based on PCR elongation of 5′-coding sequences of five Arabidopsis expressed sequence tag (EST) clones that showed significant homology to BCA1. The open reading frame of the cDNA corresponding to ACA4 (GenBank accession no. AF200739; Fig. 1) encodes a 1,030-amino-acid residue (113-kD) polypeptide that contains all of the highly conserved domains characteristic of P-type ATPases (Møller et al., 1996; Axelsen and Palmgren, 1998; Geisler et al., 2000). ACA4 has highest overall sequence homology (84% identity) to BCA1, and 62% and 63% sequence identity to ACA1 and ACA2, respectively. ACA1 (Huang et al., 1993) and ACA2 (Harper et al., 1998; Hong et al., 1999) are Arabidopsis type IIB Ca^{2+}-ATPases localized to the plastid envelope and the ER, respectively. It is interesting that ACA4 is clearly more distant (46% identity) to ACA8, a plasma membrane-bound Arabidopsis type IIB calcium pump (Bonza et al., 2000). ACA4 has about 30% to 40% sequence identity with mammalian type IIB Ca^{2+}-ATPases but less than 25% identity to mammalian type IIA Ca^{2+}-ATPases and the Arabidopsis type IIA calcium pump ACA3/ECA1 (Liang et al., 1997; Liang and Sze, 1998).

Identification of a CaM-Binding Domain in the N Terminus of ACA4

ACA4 includes a long (168-residue) N-terminal α-helix. By sequence homology, a putative CaM-binding domain was identified in the N terminus (Ala_{19}–Leu_{43}), which seems to be conserved between these isoforms. Although CaM-binding domains are more conserved in terms of structural features (Ikura et al., 1992; Brandt and Vanaman, 1998), a high degree of homology (84% identical residues) is found to a CaM-binding peptide derived from cauliflower BCA1 (Malmström et al., 1997).

To determine if this region is involved in CaM binding, we expressed a part of the N terminus (Lys_{13}–Pro_{139}) as a glutathione *S*-transferase (GST) fusion protein. In ^{125}I-CaM overlay experiments, the fusion protein bound CaM in the presence of 500 μM calcium, but not in the presence of 2 mM EGTA (pH 5.5; see Fig. 2A). GST alone did not bind CaM, neither in the presence nor in the absence of calcium. CaM interaction was confirmed by fluorescence experiments using dansyl-CaM; fluorescence of the dansyl-CaM was enhanced upon addition of fusion protein (but not with the control GST [result not shown]) in a calcium-dependent manner (see Fig. 2B).

ACA4 Is Localized to Small Vacuoles

To determine the cellular localization of ACA4, Arabidopsis microsomal membranes were separated by aqueous two-phase partitioning and the fractions obtained were probed against anti-ACA4N27. Efficient partitioning of internal membranes to the bottom phase and plasma membranes to the top phase was ascertained by western blots using marker antisera against the vacuolar V-ATPase (subunit B; Manolson et al., 1988) and the plasma membrane H^+-ATPase isoform AHA3 (Pardo and Serrano, 1989). These blots showed very little contamination of the membrane types (see Fig. 3A). The polyclonal antiserum anti-ACA4N27 was raised against a part of the N-terminal stretch of ACA4 (Lys_{13}–Pro_{139}) fused to GST and immunopurified against pure fractions of ACA4 obtained from Ni^{2+} affinity chromatography. Anti-ACA4N27 detected protein bands of the expected size in the bottom phase and in the top phase. However, only in the bottom phase could a band of approximately 110 kD be labeled that had the exact apparent molecular mass as ACA4 expressed in yeast. Additional bands in the bottom phase (around 120 kD) and top phase (around 116 kD) could represent cross-reaction with similar Ca^{2+}-ATPase isoforms.

To get more insight into the cellular localization of ACA4, Arabidopsis microsomal membranes were separated according to density by centrifugation through a linear Suc gradient (Fig. 3B). ACA4 did localize in the gradient to the same fractions as the vacuolar V-ATPase but did not colocalize with the plasma membrane marker AHA3, BIP, an ER marker, or the thylakoid marker chlorophyll.

To confirm the intracellular localization of ACA4, a fusion between ACA4 and green fluorescent protein (GFP) was constructed at the DNA level. The in vivo GFP fusion technique for intracellular localization of proteins is superior to immunological methods, based on antibodies derived from the protein, because misleading results caused by cross-

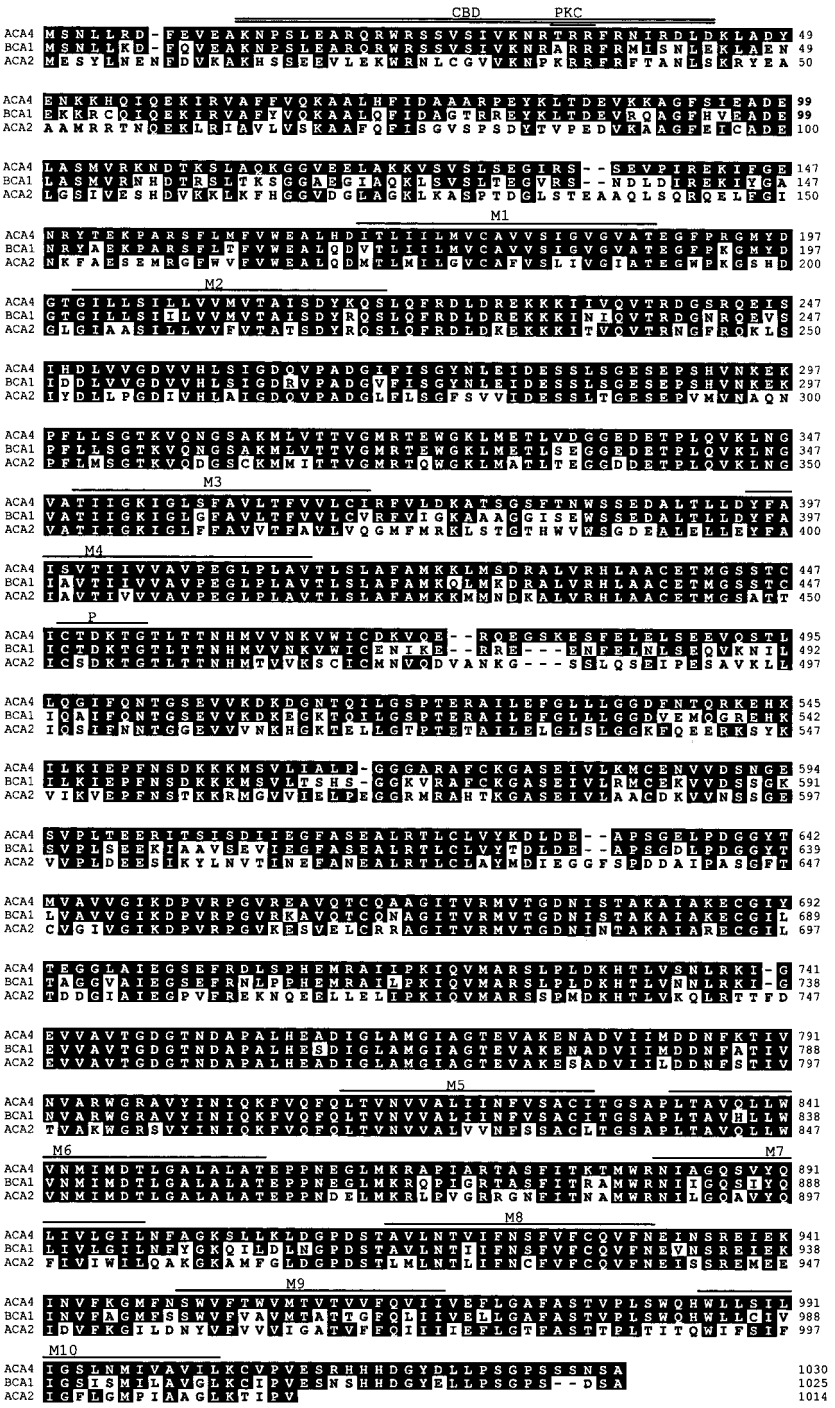

Figure 1. Sequence alignment of deduced amino acid sequences of Arabidopsis Ca^{2+}-ATPase isoform ACA4 with ACA2 and cauliflower BCA1. Sequences were aligned by the Jotun-Hein method (PAM250 comparison) using the MEGALIGN program (DNAstar, Inc., Madison, WI). Identical residues are shaded; gaps introduced to maximize alignment are denoted by hyphens. The 10 putative transmembrane domains (M1–M10) predicted using the SOAP programs are overlined. Double lines indicate a putative CaM-binding domain (CBD). PKC indicates a sequence recognition motif for protein kinase C. The ACA4 cDNA sequence reported here has the GenBank accession number AF200739 and is identical to the extracted sequence of the genomic clone (AC002510).

contamination of closely related isoforms are avoided (Geisler et al., 2000). In addition to the full-length enzyme, an N-terminal truncated variant was engineered lacking the first 47 amino acids including the putative CaM-binding auto-inhibitory domain. We added GFP to the C terminus of ACA4 because a C-terminal tag had already been shown not to alter the intracellular location of H^+-ATPase isoforms AHA3 (DeWitt and Sussman, 1995) and the calcium pump ACA2 (Hong et al., 1999). A GFP fusion to the short C terminus (which has as yet no assigned function) rather than to the auto-inhibitory N terminus seemed more appropriate in terms of both correct intracellular targeting and maintenance of physiological function.

We were unable to detect any GFP fluorescence in stable, transformed Arabidopsis seedlings, although transcription could be shown by reverse transcriptase (RT)-PCR using a pair of GFP-specific primers (data not shown). However, when these same con-

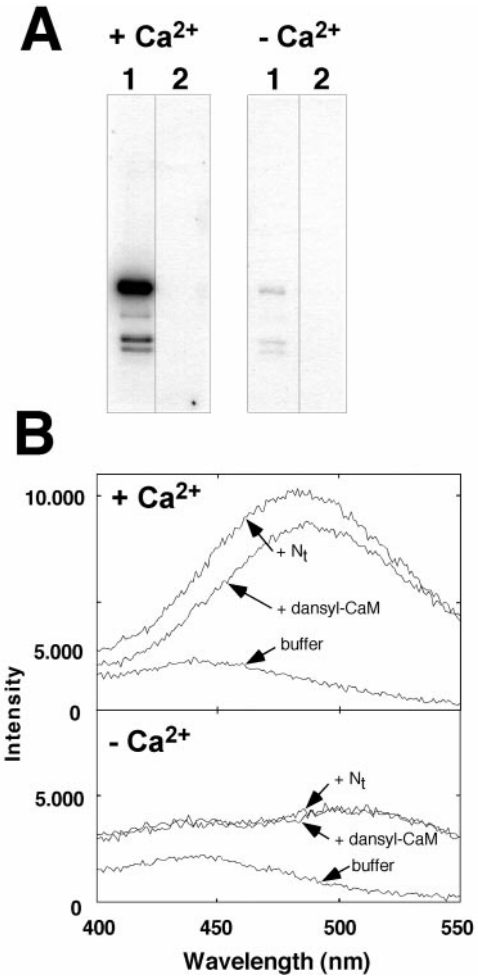

Figure 2. The N-terminal domain of ACA4 binds CaM. A, The purified fusion protein ACA4N27 (covering K_{13}–P_{139} of the ACA4 N terminus; lane 1) or the GST protein (lane 2) was blotted onto nitrocellulose and incubated with ^{125}I-CaM in the presence of 500 μM $CaCl_2$ (+Ca) or 2 mM EGTA (−Ca). After washing, blots were exposed to a phosphor-imager. B, Forty nanomolar dansyl-CaM was titrated with equimolar amounts of fusion protein (N_t) in the presence of 333 μM $CaCl_2$ (+Ca) or 2.5 mM EGTA (−Ca). Fluorescence intensity was measured by a 400- to 550-nm scan upon excitation at 340 nm in a fluorescence spectrophotometer.

structs were expressed in Arabidopsis protoplasts, fluorescence of the expressed ACA4 was detected in the periphery of small vesicles. Fluorescence was not associated with other membrane compartments like the Golgi and the plasma membrane, nor was it associated with the large central vacuole (see Fig. 4A). The full-length and the N-terminally truncated version of ACA4 seem to reside in the same compartments (Fig. 4, A and C). The size (around 2–3-μm diameter) and the density of the vesicles in comparison with the large vacuole make a vacuolar origin likely. It is interesting that the distribution of ACA4-targeted GFP fluorescence in the vacuolar membranes is not homogenous but seems to be concentrated in certain regions pointing to an unequal distribution of ACA4 in those vacuoles. In non-transformed protoplasts, a GFP signal was not detectable (results not shown). In the GFP control, the fluorescence mainly accumulates in the nucleus (see Fig. 4F) in line with previous reports on GFP localization in Arabidopsis cells (Haseloff et al., 1997).

Plant cell vacuoles have several functions, among which are storage and proteolysis of proteins (Neuhaus and Rogers, 1998). The putative water channels α-TIP and γ-TIP have been used as markers for protein storage vacuoles and lytic vacuoles, respectively (Paris et al., 1996; Vitale and Raikhel, 1999). We immunoprobed transformed protoplasts with antisera directed against γ-TIP and examined the protoplasts using immunofluorescence microscopy. In addition to the large vacuoles, radish anti-γ-TIP immunolabeled small vacuoles with a similar size and distribution compared with those showing GFP fluorescence (Fig. 4D). This result verifies the tonoplast location of ACA4.

In a minor fraction of protoplasts, ACA4-targeted GFP fluorescence was found in ER-like structures (Fig. 4E). Those protoplasts probably represent earlier stages of the secretory transport of ACA4 from the ER to the vacuolar compartments. Two days after transformation, ACA4-GFP fluorescence was found in many compartments including the ER and vacuoles, most probably due to an overloading of the secretory machinery (results not shown).

Expression of ACA4 in Arabidopsis

ACA4-specific transcripts in Arabidopsis were monitored by RT-PCR amplification of a 561-bp cDNA fragment. To circumvent problems arising from genomic DNA contamination, primers for ACA4 were chosen to cover an intron-spanning region (intron 3). ACA4-specific transcripts were found in all Arabidopsis tissues examined (see Fig. 5A) with high steady-state levels obtained from roots. Furthermore, we immunoprobed total protein extracts from those tissues prepared with anti-ACA4N27 (data not shown), confirming that ACA4 is expressed mainly in roots.

To test for the effect of external factors on ACA4-specific transcripts we used a semiquantitative RT-PCR approach. The response of the plant toward salt stress was chosen as a subject for study because Ca^{2+} has been implicated to play a role in salinity tolerance. Arabidopsis seedlings treated with different amounts of NaCl for 24 h showed a dose-dependent increase in ACA4 mRNA (see Fig. 5B). Relative amounts of ACA4 messenger reached a maximum at 100 mM NaCl (190% compared with the untreated control), whereas treatment with 200 mM NaCl lead to reduced transcript levels for both ACA4 and actin Aac1.

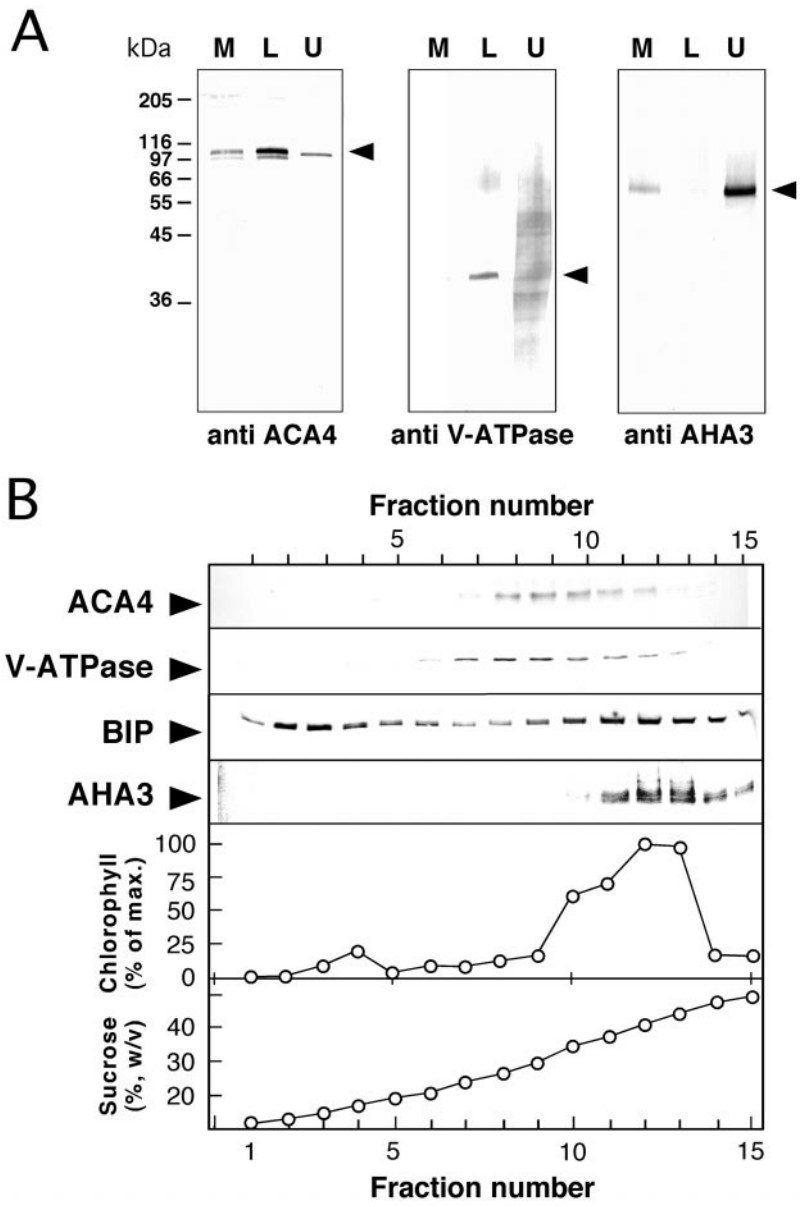

Figure 3. ACA4 is localized to internal membranes. A, To determine the intracellular localization of ACA4, microsomal fractions obtained from aqueous two-phase partitioning of root microsomes were probed with anti-ACA4N27. Efficient partitioning of the microsomes (M) to the lower (L) or to the upper (U) phase was ascertained by western blots using marker antisera against subunit B of the vacuolar V-ATPase (Manolson et al., 1988) and the plasma membrane-bound H^+-pump isoform AHA3 (Pardo and Serrano, 1989). B, Arabidopsis root microsomes subjected to Suc density gradient fractionation. Each fraction was immunoprobed with anti-ACA4N27, anti-V-ATPase (vacuolar membrane marker; Ward et al., 1992), BIP (ER marker), and anti-AHA3 (plasma membrane marker, see above). In addition, chlorophyll and Suc in the fractions were quantified.

An N-Terminally Modified Form of ACA4 Complements a Mutant of *Saccharomyces cerevisiae* Devoid of Ca^{2+}-ATPases

ACA4 was expressed both as a full-length and an N-terminally truncated enzyme in the *S. cerevisiae* triple mutant strain K616 (Cunningham and Fink, 1994). K616 lacks both endogenous Ca^{2+}-ATPases (PMR1 and PMC1), as well as the calcineurin regulatory subunit B (CNB1), and grows very poorly on low-calcium media (Cunningham and Fink, 1994; Liang et al., 1997; Harper et al., 1998). In complementation tests, it was found that ACA4 did not confer growth of K616 on low-calcium medium (Fig. 6). On the contrary, the N-terminally truncated mutants (Δ44-ACA4) supported growth of yeast under these conditions (Fig. 6), the growth rate being comparable to that of the corresponding wild type. Growth restoration was just achieved in the presence of Gal, which directly demonstrates a vector-encoded complementation.

An N-Terminally Modified Form of ACA4 Protects against Salt Stress When Expressed in *S. cerevisiae*

There is evidence that NaCl tolerance in yeast involves calcium-dependent signaling (Bressan et al., 1998). Therefore, we investigated whether Arabidopsis ACA4 expressed in the yeast mutant K616 could assume a function in these signaling events. We specifically investigated the effect of osmotic

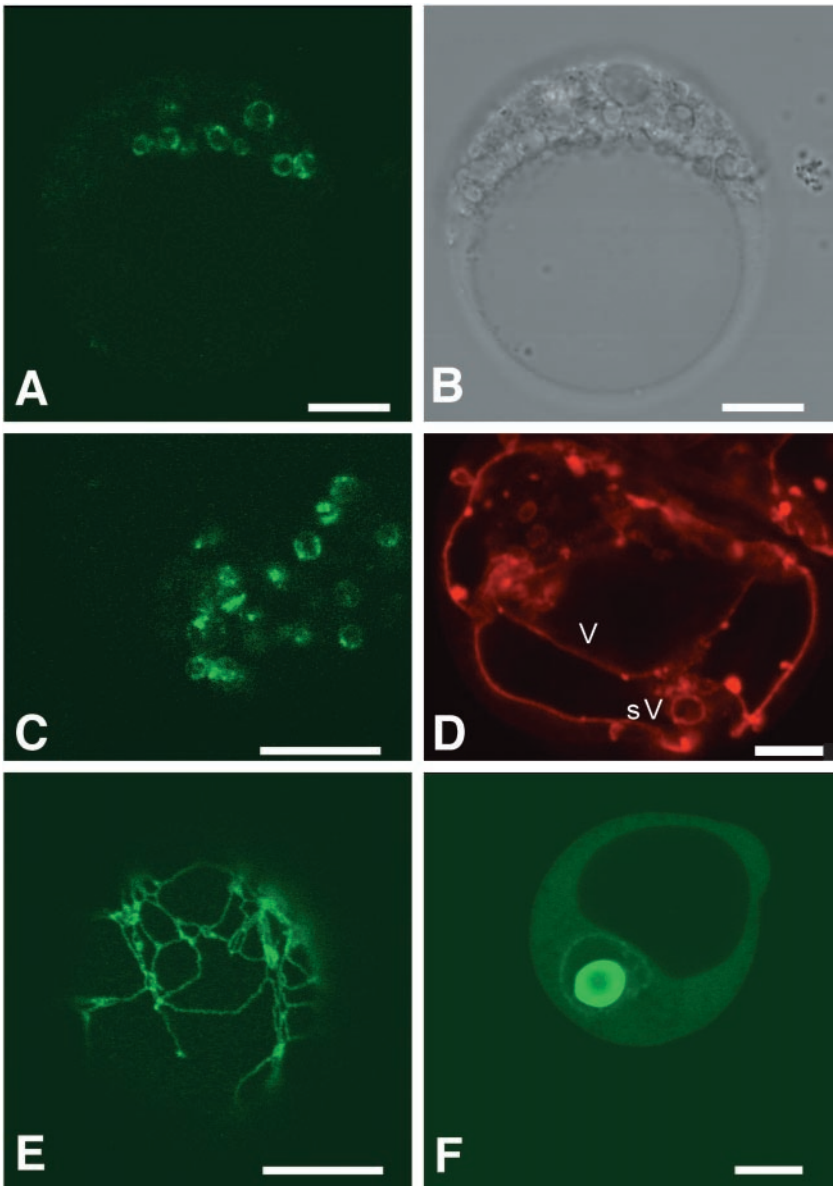

Figure 4. ACA4-GFP fluorescence is detected in small vacuoles in transiently transformed protoplasts. A, ACA4-targeted GFP fluorescence detected under blue light excitation is found in small vacuoles (sV) of transformed Arabidopsis protoplasts. B, The same sample of protoplast detected under bright field. C, GFP fluorescence of protoplasts expressing Δ47-ACA4-GFP is found in vacuoles of similar size and distribution. D, Fluorescence of transformed protoplasts immunoprobed with antisera directed against radish (*Raphanus sativus*) γ-TIP microscopy labeling the membrane of the large vacuole (V) and of small vacuoles (sV). E, In a minor fraction of protoplasts, imaging of ACA4-GFP revealed ER-like structures. F, Confocal fluorescence image of protoplast expressing GFP alone. Arabidopsis protoplasts were transformed with plasmids p35S-ACA4-GFP, p35S-Δ47-ACA4-GFP, and p35S-GFP-JH2 encoding for full length and an N-terminally truncated ACA4 fused to a C-terminal GFP, and for a GFP-only control, respectively. Confocal laser scanning images were recorded after 24 h and imaged for GFP (A–C, E–F) and lissamine rhodamine fluorescence-conjugated secondary antibody (D). The stored images were colored as green (GFP) or red (lissamine rhodamine) images using Adobe PhotoShop 5.5 (Adobe Systems, Mountain View, CA). Images were evaluated from hundreds of cells obtained from three independent experiments showing similar results. V, Large (central) vacuole; sV, small vacuoles; N, nucleus. Scale bars are 10 μm.

stresses such as high KCl, NaCl, and mannitol on the growth of the transgenic yeast cells.

On high calcium, expression of the yeast vacuolar Ca^{2+}-ATPase PMC1 as well as Arabidopsis ACA4 increased the sensitivity of the mutant yeast cells to osmotic stress (high KCl, NaCl, or mannitol). An N-terminally modified version of ACA4 produced the most pronounced effect (Fig. 7).

On low calcium (1 and 5 mM EGTA), the picture reversed. The mutant cells grew poorly under these conditions (Fig. 7) and the NaCl sensitivity of the cells were exacerbated as reported previously by Danielsson et al. (1996). When exposed to osmotic stress, expression of PMC1 and ACA4 stimulated growth of the mutant cells (Fig. 7). The N-terminally truncated ACA4 protein was able to restore growth on high NaCl even with very low external calcium (5 mM EGTA; Fig. 7). This effect appeared to be specific for NaCl because expression of the N-terminally modified ACA4 was less beneficial to cells subjected to high KCl and mannitol (Fig. 7).

DISCUSSION

ACA4 Is a Ca^{2+} Pump Localized to Small Vacuoles

In this study we cloned and genetically characterized ACA4, an Arabidopsis Ca^{2+}-ATPase resembling the vacuolar membrane CaM-regulated Ca^{2+}-ATPase BCA1 of cauliflower. Immunolocalization of ACA4 in intracellular membrane systems of Arabidopsis roots, cofractionation with a vacuolar membrane marker in Suc density gradients, as well as intracellular localization of the enzyme tagged with

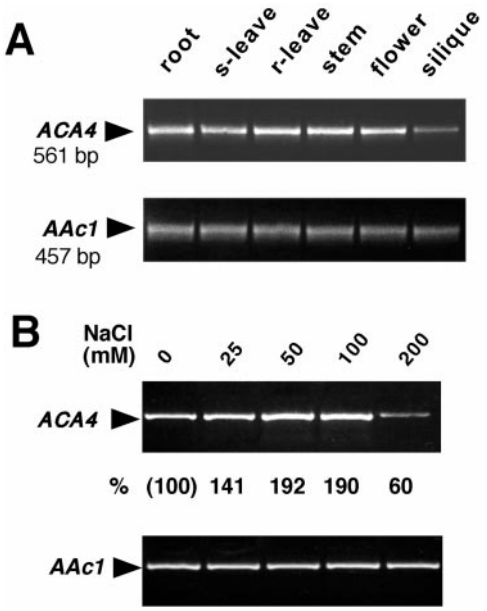

Figure 5. ACA4 expression is throughout the plant and is induced by salt stress. A, ACA4-specific transcripts (ACA4) were monitored in total RNA from different tissues by RT-PCR amplification of a 561-bp cDNA fragment. To circumvent problems with genomic DNA contamination, primers for ACA4 were chosen to cover an intron-spanning region (intron 3). As an internal control, RT-PCR on the actin Aac1 gene was employed. Control RT-PCR amplification yielded essentially constant signals (<10% deviation). B, Changes in ACA4-specific mRNA levels upon salt treatment were detected by semiquantitative RT-PCR. Arabidopsis seedlings were treated with different amounts of NaCl for 24 h, and amplified cDNA sequences were separated and quantitated. Relative intensities of the PCR bands are given in percentages as compared to control plants (no NaCl).

GFP in transiently transformed Arabidopsis protoplasts, suggest that ACA4 is situated in vacuolar membranes. It is interesting that cauliflower BCA1 seems to reside in similar vacuolar compartments, as judged from immunofluorescence microscopy data (P. Askerlund, personal communication), emphasizing the close homology between both isoforms.

ACA4 Contains an N-Terminal Auto-Inhibitory Domain

ACA4 and a mutant form devoid of the N-terminal domain (Δ44-ACA4) were introduced into the yeast *S. cerevisiae* for strain K616 (pmc1, pmr1, and cnb1) on low external calcium. This strain has been established as a genetic tool for the demonstration of calcium-pumping activity (for details, see Geisler et al., 2000) in a number of studies (Liang et al., 1997; Harper et al., 1998). In K616, both endogenous Ca^{2+}-ATPases are deleted and the regulatory subunit B (Cnb1) has been disrupted. The fact that the N-terminally truncated, but not the full-length, ACA4 Ca^{2+}-ATPase was able to complement endogenous yeast Ca^{2+}-ATPases indicates that truncation of the N-terminal region seems to transfer ACA4 into an activated state. Lack of complementation for the full-length enzyme also indicates that activation of ACA4 by endogenous yeast CaM isoforms did not occur due to reasons of incompatibility and/or to low calcium concentrations. Alternative interpretations, such as incorrect endomembrane targeting or insufficient expression levels, could be excluded because ACA4 displayed a similar expression and endomembrane distribution to that for Δ44-ACA4 (data not shown).

Overall, the regulatory features of ACA4 seem to be similar to ACA2 (Harper et al., 1998), an Arabidopsis Ca^{2+} pump localized to the ER (Hong et al., 1999). In this pump, auto-inhibitory and CaM-binding domains in the N terminus overlap within a 25-residue region (Hwang et al., 2000). It is likely that in both ACA4 and ACA2, the role of CaM is to

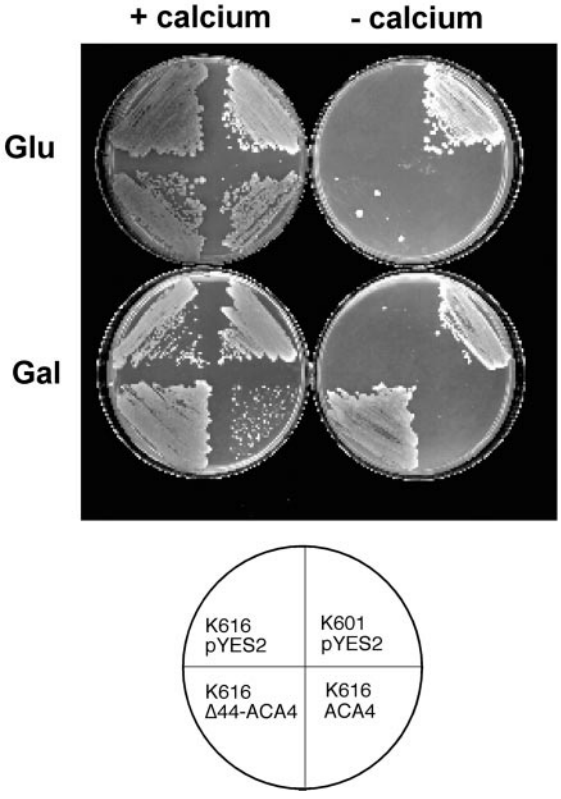

Figure 6. An N-terminally modified form of ACA4 complements a yeast strain devoid of Ca^{2+}-ATPases. Triple mutant K616 (Pmr1 Pmc1 Cnb1) strain was transformed with control vectors pYES2 (vector control), pYES2-ACA4 (ACA4), or pYES2-Δ44ACA4 (Δ44-ACA4), respectively. Single colonies were streaked out on SC-Ura/Gal or SC-Ura/Glu plates containing 10 mM Ca^{2+} (+ calcium) or 10 mM EGTA, pH 5.5 (− calcium) and incubated for 3 d at 30°C. In the presence of Gal only the N-terminal truncated ACA4 was able to provide growth of strain K616 on EGTA that was comparable to wild-type strain K601, whereas the full-length enzyme was not.

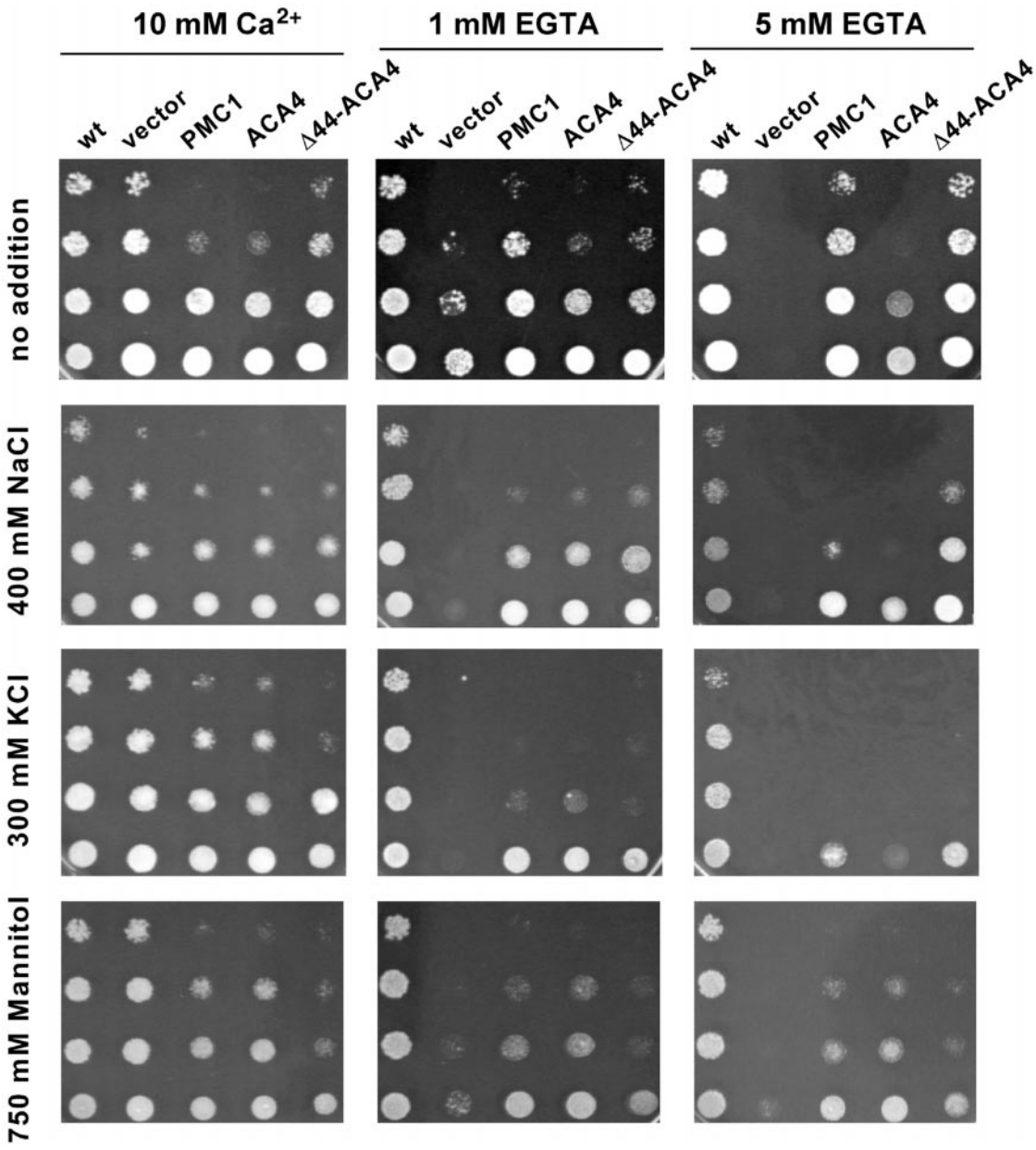

Figure 7. Effect of salinity on growth of yeast strain K616 complemented by ACA4. Triple mutant K616 (Pmr1 Pmc1 Cnb1) strain was transformed with control vectors pYES2, pYES2-PMC1 (PMC1), pYES2-ACA4 (ACA4), and pYES2-Δ44ACA4 (Δ44-ACA4), respectively. For drop tests, mid-log precultures in SC-Ura plus 10 mM $CaCl_2$ were pelleted, washed twice, and an optical density at 600 nm of 1.0 in water was obtained by dilution. Cells were diluted 10-fold and each 5 μL was spotted on SC-Ura/Gal plates supplemented with different EGTA, KCl, NaCl, or mannitol concentrations. Growth was recorded after 4 d of incubation at 30°C.

neutralize the constraint on the pumps exerted by the N terminus.

ACA4 Functions in Calcium Signaling upon Salt Stress

To assign a biological function to ACA4 we tested its involvement in calcium signaling upon salt stress. Two lines of evidence suggest that ACA4 might be part of that Ca^{2+}-dependent signal transduction pathway linked to salt stress: (a) The ACA4 transcript in Arabidopsis was increased by NaCl, and (b) when expressed in yeast, ACA4 conferred increased NaCl tolerance to its host.

ACA4-specific transcripts accumulated upon NaCl treatment, as detected by semiquantitative RT-PCR (Fig. 5B). NaCl-enhanced ACA4 expression is

in accordance with its putative role in NaCl adaptation. For type IIA Ca^{2+}-ATPases from tomato (Wimmers et al., 1992) and tobacco (Perez-Prat et al., 1992), similar results have been reported and it has been postulated that the increase in cytosolic Ca^{2+} upon NaCl exposure might be lowered by an increased capacity of calcium pumps (Niu et al., 1995). Because ACA4 is a type IIB Ca^{2+}-ATPase, both the IIA and IIB subtypes of plant calcium pumps seem to be involved in similar pathways upon salt stress. NaCl induction of IIA Ca^{2+}-ATPases detected by northern blot was severalfold stronger as compared with the induction of ACA4 detected via RT-PCR. Differences in induction levels might reflect functional differences between both subtypes. It is interesting that expression of the putative Arabidopsis vacuolar Ca^{2+}/H^{+} antiporter CAX1 is also only weakly stimulated by NaCl (Hirschi, 1999).

Yeast has provided us with a model to study Ca^{2+} signaling upon salt stress (Bressan et al., 1998; Piao et al., 1999). *S. cerevisiae* strain K616, which in addition to calcineurin is deficient in calcium pumps, is NaCl-sensitive resulting mainly from loss of calcineurin-induced expression of the ENA1/PMR2a Na^{+} pump (Danielsson et al., 1996). In addition, due to the lack of calcineurin in this strain, the activity of the vacuolar membrane H^{+}/Ca^{2+} exchanger VCX1 is high (Cunningham and Fink, 1994). In the presence of high external calcium, cytosolic concentrations of calcium are probably high enough for the low-affinity transporter VCX1 to be active, allowing it to transport calcium into the vacuole. However, at low external calcium concentrations, VCX1 is likely to be less active. Under these conditions, expression of high-affinity calcium pumps becomes important for filling internal calcium stores.

Expression of Arabidopsis ACA4 conferred some osmoprotection when expressed in the yeast triple mutant strain K616. The yeast vacuolar membrane Ca^{2+}-ATPase PMC1, which is transcriptionally controlled by calcineurin (Cunningham and Fink, 1996), had almost the same effect. This outcome would suggest that any Ca^{2+}-ATPase functioning at the yeast vacuole suppresses the osmosensitive phenotype of K616.

Expression of the N-terminally truncated ACA4, which is deregulated, almost ameliorated NaCl hypersensitivity of the K616 strain. The fact that the mutant version of ACA4 provided substantially more salt tolerance than the full-length enzyme might be explained by a more efficient filling of small endomembrane calcium stores in the mutant. Activation of the pump by endogenous CaM apparently seems not to be as effective in creating an activated pump as N-terminal truncation. This finding is in line with biochemical data on purified reconstituted ACA4 showing that the specific Ca^{2+}-ATPase activity of the truncated enzyme is severalfold higher when compared with that of the CaM-activated enzyme (M. Geisler and M.G. Palmgren, unpublished data). N-terminally truncated mutants of Arabidopsis isoform ACA2 (Harper et al., 1998; Hwang et al., 2000) and cauliflower BCA1 (Malmström et al., 2000) are also more active than the corresponding full-length enzymes in the presence of calcium/CaM.

It is interesting that under conditions of high external calcium, where VCX1 is supposed to be active, expression of calcium pumps was not beneficial; rather, increased stress sensitivity was the result (Fig. 7). In line with these results, it has been observed that expression in tobacco of CAX1, a putative Arabidopsis H^{+}/Ca^{2+} exchanger, causes increased stress sensitivity (Hirschi, 1999).

CONCLUSION

In summary, our results indicate that ACA4, a novel member of the subfamily of N-terminal CaM-regulated Ca^{2+}-ATPases, is situated in the membrane of small vacuoles of Arabidopsis. The putative involvement of ACA4 in calcium signaling upon NaCl stress is of special interest. Because it now seems likely that an increase in cytosolic Ca^{2+} concentration caused by NaCl is indeed an effector of salt tolerance, elevated calcium levels must be transitory. Thus ACA4 (together with vacuolar H^{+}/Ca^{2+} antiporters like Arabidopsis CAX1 [Hirschi et al., 1996]) might adjust cytosolic calcium concentrations by filling vacuolar compartments, the major plant calcium storage organelles (Bush, 1995; Muir and Sanders, 1997).

By overexpression of the vacuolar Na^{+}/H^{+} antiporter AtNHX1 (Apse at al., 1999; Gaxiola et al., 1999) salt tolerance in Arabidopsis can be achieved by direct compartmentalization of sodium away from the cytosol (Apse at al., 1999). Here we provide evidence that, at least in yeast, salt tolerance might also be achieved indirectly via the reestablishment of intracellular calcium levels. The nature of calcium spikes is believed to be important for the cell to interpret their information content. In this context, the activity of calcium pumps might be important for controlling the amplitude and frequency of such spikes (Sze et al., 2000). We propose that during conditions of osmotic stresses, when intracellular calcium is expected to increase, high-affinity calcium pumps are important for the rapid refilling of intracellular calcium stores, in this way contributing to the generation of a calcium signal that results in the appropriate stress response.

MATERIALS AND METHODS

Cloning of ACA4 cDNA

ACA4 cDNA was isolated by elongating 5′ coding sequences of ESTs using nested PCR amplification of Arabidopsis cDNA. Using cauliflower (*Brassica oleracea*) BCA1 cDNA (Malmström et al., 1997), The Institute for Genomic Research's (Rockville, MD) nonredundant EST database (http://www.tigr.org) was searched to identify putative Arabidopsis homologues of BCA1. EST W43599, T41650, N96705, R65015, N65090, and T43417 were obtained from the Arabidopsis Biological Research Center (Ohio State University, Columbus) and sequenced. 5′ ends of T41650, N96705, N65090, R65015, and T43417 were elongated by nested PCR similar to that described by Mundy et al. (1995). cDNA of the size-fractionated (3–6 kb) library CD4-16 (Kieber et al., 1993) in λ ZAPII (Stratagene, La Jolla, CA) was used as a template. The longest PCR products of each reaction (ranging from 1.5–2.4 kb, respectively) were sub-cloned into the T vector pT7blue (Novagen, Madison, WI). The 1.9 kb of clone pT7-A4 fragments obtained from N65090 showed the highest homology to BCA1. The missing 5′ portion was obtained by an additional nested PCR amplification of a 400-bp fragment from Arabidopsis cDNA using conditions as described above.

For sub-cloning of the entire gene, a long-range nested PCR on cDNA derived from library CD4-16 was performed as described above using the *Taq*$^+$ Precision system (Stratagene). The nested primers were designed to contain restriction sites for directional cloning; additionally, the primer matching the 5′ end contained a sequence coding for a C-terminal $RGSH_6$ motif enabling western detection and purification by Ni^{2+}-affinity chromatography. A 5′-truncated cDNA lacking the first 44 amino acids of ACA4 also was generated by PCR, introducing a point mutation converting Lys_{45} into Ser_2. PCR-generated cDNA was directionally cloned into the *Kpn*I and *Xho*I sites of the yeast-*Escherichia coli* shuttle vector pYES-2 (Invitrogen, Carlsbad, CA), setting expression of ACA4 under the control of the Gal-dependent Gal1 promoter, and resulting in the plasmids pYES2-ACA4, pYES2-Δ44ACA4, pYES2-ACA4-H6, and pYES2-Δ44ACA4-H6.

Expression and Purification of the ACA4 N Terminus and Antiserum Production

A 435-bp fragment encoding Lys_{13} through Pro_{139} of ACA4 was amplified by PCR under standard conditions using the plasmid pT7-A4 as a template. The cDNA was cloned into the *E. coli* expression vector pGEX-4T-1 (Pharmacia Biotech, Piscataway, NJ) opened with *Eco*RI and *Xho*I leading to an N-terminal fusion with GST and a C-terminal 6x-His tag (pGEX-N27). The expressed N-terminal stretch of ACA4 was purified by Ni^{2+}-affinity chromatography under denaturating conditions as described by Geisler et al. (1998).

Rabbit polyclonal anti-ACA4 antisera (anti-ACA4N27) were produced at the Statens Serum Institut (Copenhagen). Purified fusion protein ACA4N27 was injected subcutaneously into rabbits following standard protocols. Antisera were purified by caprylic acid and ammonium sulfate precipitation followed by immunopurification against purified ACA4. Anti-GST was removed by applying the antisera onto a column containing affi-10 (Bio-Rad Laboratories, Hercules, CA) coupled to purified GST, as recommended by the manufacturer. The flow-through was loaded onto a column containing purified 6x-His-tagged ACA4 immobilized with affi-10, eluted with 0.1 M Gly (pH 2.4), and dialyzed against phosphate-buffered saline.

CaM-Binding Studies

The purified 42-kD fusion protein was subjected to 10% (w/v) SDS-PAGE, blotted onto nitrocellulose membranes coated with 2% (w/v) bovine serum albumin in Tris-buffered saline (10 mM Tris-HCl, pH 7.4, and 150 mM NaCl) and probed with bovine brain CaM (Sigma, St. Louis) ^{125}I-iodinated using Bolter and Hunter reagent (Amersham, Buckinghamshire, UK) as described in Malmström et al. (1997). Blots incubated overnight with ^{125}I-CaM in the presence or absence of $CaCl_2$ or EGTA were washed with TNT (Tris-buffered saline plus 0.05% [v/v] Tween 20) plus 500 μM $CaCl_2$ or 2 mM EGTA for 3 h with several buffer changes and were exposed to a phosphor-imager.

CaM binding of the expressed ACA4 N terminus alternatively was investigated in fluorescence experiments using dansyl-CaM as described in Carafoli et al. (1992). Here 40 nM dansyl-CaM was pre-incubated in 20 mM HEPES [4-(2-hydroxyethyl)-1-piperazineethanesulfonic acid] and 130 mM KCl (total volume of 3 mL) in the presence of 333 μM $CaCl_2$ or 2.5 mM EGTA. Fluorescence intensity was measured by a 400- to 550-nm scan in a fluorescence spectrophotometer (Shimadzu, Columbia, MD) upon excitation at 340 nm and titration with equimolar amounts of fusion protein or GST.

Yeast Transformation, Complementation, and Growth

After confirmation of the fidelity of the constructs by sequencing, yeast strains K601/W3031A (MATa, leu2, his3, ade2, and ura3), and K616 (MATa pmr1::HIS3 pmc1::TRP1 cnb1::LEU2 and ura3; Cunningham and Fink, 1994) were transformed with plasmids pYES2-ACA4, pYES2-Δ44ACA4, pYES2-PMC1, or the empty pYES2 vector, respectively. Transformants were selected for uracil prototrophy by plating on synthetic media lacking uracil (SC-Ura). Ura+ colonies were grown in medium containing 2% (w/v) Glc or Gal, 50 mM succinic acid/Tris (pH 5.5) plus 0.7% (w/v) yeast nitrogen base supplemented with the required amino acids at 30 μg/mL at 30°C. Strain K616 was grown in the presence of 10 mM $CaCl_2$.

For complementation experiments, single colonies were transferred in 500 μL of sterile water and streaked on SC-Ura/Gal and SC-Ura/Glu plates containing either 10 mM $CaCl_2$ or 10 mM EGTA (pH 5.5). To monitor growth of

mutant yeast strains complemented by ACA4, drop tests were performed. Mid-log precultures in SC-Ura plus 10 mM $CaCl_2$ were pelleted, washed twice, and an optical density at 600 nm of 1.0 in water was obtained by volume adjustment. Cells were serially diluted 10-fold three times and 5 μL of each dilution was spotted on SC-Ura/Gal plates supplemented with different concentrations of $CaCl_2$ (0 and 10 mM $CaCl_2$ and 1, 5, and 10 mM EGTA), NaCl (0, 100, 200, 400, and 800 mM), LiCl (0, 10, 20, 40, and 80 mM), KCl (0, 75, 150, 300, and 600 mM), and mannitol (0, 250, 500, 750, and 1000 mM). Growth was recorded after 3 to 5 d of incubation at 30°C.

Detection of ACA4-Specific Transcripts by RT-PCR

Arabidopsis total RNA, either from different plant tissues of soil-grown plants or from seedlings grown in liquid cultures under mixotrophic conditions (1× Murashige and Skoog medium, 1% [w/v] Suc; constant light) for 7 d, was prepared using the RNeasy Plant Kit (Qiagen USA, Valencia, CA). For salt treatments, various amounts of NaCl were added to the liquid cultures and seedlings were collected after 24 h grown in the dark to reduce starch accumulation.

ACA4- and actin1 (AAc1)-specific transcripts (EMBL/GenBank/DNA data bank of Japan accession no. M20016) were detected by RT-PCR using either the rTth RNA-Polymerase kit (Perkin-Elmer Applied Biosystems, Foster City, CA) or the Titan One-tube RT-PCR kit (Boehringer Mannheim, Basel) according to the instructions given by the manufacturer. Each reaction contained up to 200 ng (ACA4) or 50 ng (AAc1) total RNA; PCR reactions were run for 30 cycles at 58°C. Equal volumes of PCR product were separated on 3% (w/v) agarose gels and the ethidium bromide fluorescence was quantitated using the Scion Image software (version 3.62a; http://www.scioncorp.com). Intron-spanning sense (S) and anti-sense (AS) RT-PCR primers used were: Aac1-S: 5′-GTG CTC GAC TCT GGA GAT GGT GTG-3′, Aac1-AS: 5′-CGG CGA TTC CAG GGA ACA TTG TGG-3′, ACA4-S: 5′-GGC ATC GTT TGT CCC ATC CCC-3′, and ACA4-AS: 5′-GGT GGT GCA CGG GCT TTC TGC-3′. Negative controls in the absence of enzyme in the reverse transcription step were run and yielded no products. The relative intensities in different lanes within each single experiment were independent of the number of PCR cycles performed.

Membrane Fractionation

Microsomal membranes were isolated from Arabidopsis tissue grown in liquid cultures under mixotrophic conditions (see above) as described in Sidler et al. (1998). Vesicles were finally resuspended in STED10 (10% [w/v] Suc in STED [100 mM Tris-HCl {pH 7.5}, 1 mM EGTA, and 1 mM dithiothreitol]) and loaded onto a 10% to 50% (w/v) continuous Suc gradient of the same buffer composition. Gradients were centrifuged at 100,000*g* for 15 h and 1-mL fractions were collected. Aliquots of equal volume were blotted on nitrocellulose and probed with anti-ACA4 (anti-ACA4N27: 1: 1000, this work), anti-AHA3 (no. 762: 1: 3000, Pardo and Serrano, 1989), anti-V-ATPase (2E7: 1: 200, Ward et al., 1992) and anti-BIP (tobacco [*Nicotiana tabacum*] BIP: 1: 5000). A refractometer was used to measure Suc concentrations and chlorophyll a and b content was determined spectrophotometrically in ethanol using the equation $C_{a+b} = 5.24\ A_{664.2} + 22.24\ A_{646.6}$.

Protoplast Transformation

Arabidopsis protoplasts were isolated and transformed as described by Negrutia et al. (1987) and Di Sansebastiano et al. (1998) with minor modifications. A 200-mL aliquot of a 4-d-old cell suspension culture (cell line T87; Axelos et al., 1992) was filtered through a 50-μm nylon sieve and the cells collected were incubated for 3 h in culture medium containing 1% (w/v) cellulase and 0.4% (w/v) Macerozyme R10. Protoplasts were purified according to the protocol of Nagy and Maliga (1976).

Protoplasts were transformed with the plant binary vectors p35S-ACA4-GFP and p35S-Δ47-ACA4-GFP by polyethylene glycol-mediated direct gene transfer essentially as described by Freydl et al. (1995). The plasmids p35S-ACA4-GFP and p35S-Δ47-ACA4-GFP encode full-length and an N-terminal truncated ACA4, respectively, fused to a C-terminal GFP (S65T) under the control of the cauliflower mosaic virus 35S promoter. The 35S-GFP vector p35S-GFP-JH2 (mp25) is identical to p35S-GFP-JH1 as described in Hong et al. (1999) except that it carries the *bar* gene, providing resistance against the herbicide glufosinate ammonium (BASTA, Hoechst, Frankfurt). ACA4, both as a full-length and N-terminal truncated enzyme, was sub-cloned into the *Spe*I site of vector p35S-GFP-JH2 using long-range PCR as described above; *Spe*I sites were introduced in-frame into the 5′ ends of the PCR primers.

Immunocytochemistry and Confocal Fluorescence Microscopy Analysis

Confocal immunofluorescence localization was performed on permeabilized cells as described in Paris et al. (1996). Arabidopsis transiently transformed protoplasts were fixed for at least 24 h in 3.7% (w/v) formaldehyde in 50 mM HEPES and 0.5 M mannitol (pH 7.0). Cell membranes were permeabilized by a 5-min treatment in 0.5% (w/v) Triton X-100. After blocking with 1% (w/v) bovine serum albumin, 0.25% (w/v) gelatin, 0.05% (w/v) Nonidet P40, and 0.02% (w/v) sodium azide in phosphate-buffered saline, protoplasts were incubated for 1 h with anti-radish (*Raphanus sativus*) γ-TIPVM23 (Maeshima, 1992) at a 1/100 dilution. After three washes, protoplasts were treated for 1 h with the secondary antibody (anti-rabbit coupled to the fluorochrome lissamine rhodamine [Jackson Immunoresearch Laboratories, West Grove, PA]) at a 1/100 dilution and rinsed three times for 10 min.

Confocal images of protoplasts were recorded after 24 h after transformation with the confocal laser microscope

DMR using the TCS 4D operating system (Leica Microsystems, Wetzlar, Germany). GFP and lissamine rhodamine fluorescence were detected with the filter set for fluorescein isothiocyanate and tetramethylrhodamine B isothiocyanate, respectively. The stored images were colored as green (GFP) or red (lissamine rhodamine) images using Adobe PhotoShop 5.5 (Adobe Systems).

ACKNOWLEDGMENTS

We would like to thank Dr. K. Cunningham for providing us with yeast strains K601, K616, and plasmid pKC151, Dr. P. Askerlund for help in performing CaM overlay experiments and anti V-ATPase antibody (Manolson et al., 1988), Dr. T. Jahn for Arabidopsis root microsome fractions, Dr. H. Sze for anti V-ATPase, Dr. A. Vitale for anti-BIP, and Dr. J. Harper for the plant binary vector p35S-GFP-JH2.

Received May 17, 2000; modified July 2, 2000; accepted September 12, 2000.

LITERATURE CITED

Allen GJ, Muir SR, Sanders D (1995) Release of Ca^{2+} from individual plant vacuoles by both $InsP_3$ and cyclic ADP-ribose. Science **268:** 735–737

Apse MP, Aharon GS, Snedden WA, Blumwald E (1999) Salt tolerance conferred by overexpression of a vacuolar Na^+/H^+ antiport in Arabidopsis. Science **285:** 1256–1258

Askerlund P (1997) Calmodulin-stimulated Ca^{2+}-ATPase in the vacuolar and plasma membranes in cauliflower. Plant Physiol **114:** 999–1007

Axelos M, Curie C, Mazzolini L, Bardet C, Lescure B (1992) A protocol for transient gene expression in *Arabidopsis thaliana* protoplasts isolated from cell suspension cultures. Plant Physiol Biochem **30:** 123–128

Axelsen KB, Palmgren MG (1998) Evolution of substrate specificities in the P-type ATPases superfamily. J Mol Evol **46:** 84–101

Bonza MC, Morandina P, Luoni L, Geisler M, Palmgren MG, De Michelis MI (2000) Cloning of *At*-ACA8, a plasma membrane-localized, calmodulin-regulated Ca^{2+}-ATPase of Arabidopsis and localization of its calmodulin-binding domain at the N-terminus. Plant Physiol **116:** 845–851

Brandt PC, Vanaman TC (1998) Calmodulin and ion flux regulation. *In* L Van Eldik, DM Watterson, eds, Calmodulin and Signal Transduction. USA Academic Press, San Diego, pp 397–471

Bressan RA, Hasegawa PM, Pardo JM (1998) Plants use calcium to resolve salt stress. Trends Plant Sci **3:** 411–412

Bush DS (1995) Calcium regulation in plant cells and its role in signaling. Annu Rev Plant Physiol Plant Mol Biol **46:** 95–112

Carafoli E, Kessler F, Falchetto R, Heim R, Quadroni M, Krebs J, Strehler EE, Vorherr T (1992) The molecular basis of the modulation of the plasma membrane calcium pump by calmodulin. Ann N Y Acad Sci **671:** 58–68

Cunningham KW, Fink GR (1994) Calcineurin-dependent growth control in *Saccharomyces cerevisiae* mutants lacking PMC1, a homolog of plasma membrane Ca^{2+}-ATPases. J Cell Biol **124:** 351–363

Cunningham KW, Fink GR (1996) Calcineurin inhibits VCX1-dependent H^+/Ca^{2+} exchange and induces Ca^{2+}-ATPases in *Saccharomyces cerevisiae*. Mol Cell Biol **16:** 2226–2237

Danielsson A, Larsson C, Larsson K, Gustafsson L, Adler L (1996) A genetic analysis of the role of calcineurin and calmodulin in Ca^{++}-dependent improvement of NaCl tolerance of *Saccharomyces cerevisiae*. Curr Genet **30:** 476–484

DeWitt ND, Sussman MR (1995) Immunocytological localization of an epitope-tagged plasma membrane proton pump (H^+-ATPase) in phloem companion cells. Plant Cell **7:** 2053–2067

Di Sansebastiano GP, Paris N, Marc-Martin S, Neuhaus J-M (1998) Specific accumulation of GFP in a non-acidic vacuolar compartment via a C-terminal propeptide-mediated sorting pathway. Plant J **15:** 449–457

Ehrhardt DW, Wais R, Long SR (1996) Calcium spiking in plant root hairs responding to *Rhizobium* nodulation signals. Cell **85:** 673–681

Epstein E (1998) How calcium enhances plant salt tolerance. Science **280:** 1906–1907

Evans DE, Williams LE (1998) P-type calcium ATPases in higher plants: biochemical, molecular and functional properties. Biochim Biophys Acta **9:** 1–25

Freydl E, Meins F Jr, Boller T, Neuhaus JM (1995) Kinetics of prolyl hydroxylation, intracellular transport and C-terminal processing of the tobacco vacuolar chitinase. Planta **147:** 250–256

Gaxiola RA, Rao R, Sherman A, Grisafi P, Alper SL, Fink GR (1999) The *Arabidopsis thaliana* proton transporters, AtNhx1 and Avp1, can function in cation detoxification in yeast. Proc Natl Acad Sci USA **96:** 1480–1485

Geisler M, Axelsen BK, Harper JF, Palmgren MG (2000) Molecular aspects of higher plant Ca^{2+}-ATPases. Biochim Biophys Acta **1465:** 52–78

Geisler M, Koenen W, Richter J, Schumann J (1998) Expression and characterization of a *Synechocystis* PCC 6803 P-type ATPase in *E. coli* plasma membranes. Biochim Biophys Acta **1368:** 267–275

Halfter U, Ishitani M, Zhu JK (2000) The Arabidopsis SOS2 protein kinase physically interacts with and is activated by the calcium-binding protein SOS3. Proc Natl Acad Sci USA **97:** 3735–3740

Harper JF, Hong B, Hwang I, Guo HQ, Stoddard R, Huang JF, Palmgren MG, Sze H (1998) A novel calmodulin-regulated Ca^{2+}-ATPase (ACA2) from Arabidopsis with an N-terminal autoinhibitory domain. J Biol Chem **273:** 1099–1106

Haseloff J, Siemering KR, Prasher DC, Hodge S (1997) Removal of a cryptic intron and subcellular localization

of green fluorescent protein are required to mark transgenic Arabidopsis plants brightly. Proc Natl Acad Sci USA **94:** 2122–2127

Hirschi KD (1999) Expression of Arabidopsis CAX1 in tobacco: altered calcium homeostasis and increased stress sensitivity. Plant Cell **11:** 2113–2122

Hirschi KD, Zhen RG, Cunningham KW, Rea PA, Fink GR (1996) CAX1, an H^+/Ca^{2+} antiporter from Arabidopsis. Proc Natl Acad Sci USA **93:** 8782–8786

Hong B, Ichida A, Wang Y, Gens JS, Pickard B, Harper JF (1999) Identification of a calmodulin-regulated Ca^{2+}-ATPase in the endoplasmic reticulum. Plant Physiol **119:** 1165–1176

Huang L, Berkelman T, Franklin AE, Hoffman NE (1993) Characterization of a gene encoding a Ca^{2+}-ATPase-like protein in the plastid envelope. Proc Natl Acad Sci USA **90:** 10066–10070

Hwang I, Harper JF, Liang F, Sze H (2000) Calmodulin activation of an endoplasmic reticulum-located calcium pump involves an interaction with the N-terminal autoinhibitory domain. Plant Physiol **122:** 157–168

Ikura M, Clore GM, Groneborn AM, Zhu G, Klee CB, Bax A (1992) Solution structure of a calmodulin-target peptide complex by multidimensional NMR. Science **256:** 632–638

Jaffe LF, Creton R (1998) On the conservation of calcium wave speeds. Cell Calcium **24:** 1–8

Jang HJ, Pih KT, Kang SG, Lim JH, Jin JB, Piao HL, Hwang I (1998) Molecular cloning of a novel Ca^{2+}-binding protein that is induced by NaCl stress. Plant Mol Biol **37:** 839–847

Kieber JJ, Rothenberg M, Roman G, Feldmann KA, Ecker JR (1993) CTR1, a negative regulator of the ethylene response pathway in Arabidopsis, encodes a member of the Raf family of protein kinases. Cell **72:** 427–441

Liang F, Cunningham KW, Harper JF, Sze H (1997) ECA1 complements yeast mutants defective in Ca^{2+} pumps and encodes an endoplasmic reticulum-type Ca^{2+}-ATPase *in Arabidopsis thaliana*. Proc Natl Acad Sci USA **5:** 579–584

Liang F, Sze H (1998) A high-affinity Ca^{2+} pump, ECA1, from the endoplasmic reticulum is inhibited by cyclopiazonic acid but not by thapsigargin. Plant Physiol **118:** 817–825

Liu J, Zhu JK (1997) An Arabidopsis mutant that requires increased calcium for potassium nutrition and salt tolerance. Proc Natl Acad Sci USA **94:** 14960–14964

Liu J, Zhu JK (1998) A calcium sensor homolog required for plant salt tolerance. Science **280:** 1943–1945

Maeshima M (1992) Characterization of the major integral protein of vacuolar membrane. Plant Physiol **98:** 1248–1254

Malmström S, Åkerlund H-E, Askerlund P (2000) Regulatory role of the N-terminus of the vacuolar Ca^{2+}-ATPase in cauliflower. Plant Physiol **122:** 517–526

Malmström S, Askerlund P, Palmgren MG (1997) A calmodulin-stimulated Ca^{2+}-ATPase from plant vacuolar membranes with a putative regulatory domain at its N-terminus. FEBS Lett **6:** 324–328

Manolson MF, Ouellette BF, Filion M, Poole RJ (1988) cDNA sequence and homologies of the "57-kDa" nucleotide-binding subunit of the vacuolar ATPase from Arabidopsis. J Biol Chem **263:** 17987–17994

McAinsh MR, Brownlee C, Hetherington AM (1997) Calcium ions as second messenger in guard cell signal transduction. Physiol Plant **100:** 16–29

McAinsh MR, Hetherington AM (1998) Encoding specificity in Ca^{2+} signaling systems. Trends Plant Sci **3:** 32–36

Møller JV, Juul B, Le Maire M (1996) Structural organization, ion transport, and energy transduction of P-type ATPases. Biochim Biophys Acta **1286:** 1–51

Muir SR, Sanders D (1997) Inositol 1,4,5-triphosphate-sensitive Ca^{2+} release across nonvacuolar membranes in cauliflower. Plant Physiol **114:** 1511–1521

Mundy J, Mayer R, Chua N-H (1995) Cloning genomic sequences using long-range PCR. Plant Mol Biol Rep **13:** 156–163

Nagy JI, Maliga P (1976) Callus induction and plant regeneration from mesophyll protoplasts of *Nicotiana sylvestris*. Z Pflanzenphysiol **78:** 453–455

Negrutia I, Shillito RD, Potrykus I, Biasini G, Sala F (1987) Hybrid genes in the analysis of transformation conditions: I. Setting up a simple method for direct gene transfer in plant protoplasts. Plant Mol Biol **8:** 363–373

Neuhaus J-M, Rogers JC (1998) Sorting of proteins to vacuoles in plant cells. Plant Mol Biol **38:** 127–144

Niu X, Bressan A, Hasegawa PM, Pardo JM (1995) Ion homeostasis in NaCl stress environments. Plant Physiol **109:** 735–742

Pardo JM, Reddy MP, Yang S, Maggio A, Huh GH, Matsumoto T, Coca MA, Paino-D'Urzo M, Koiwa H, Yun DJ, Watad AA, Bressan RA, Hasegawa PM (1998) Stress signaling through Ca^{2+}/calmodulin-dependent protein phosphatase calcineurin mediates salt adaptation in plants. Proc Natl Acad Sci USA **95:** 9681–9686

Pardo JM, Serrano R (1989) Structure of a plasma membrane H^+-ATPase gene from the plant *Arabidopsis thaliana*. J Biol Chem **264:** 8557–8562

Paris N, Stanley CM, Jones RL, Rogers JC (1996) Plant cells contain two functionally distinct vacuolar compartments. Cell **85:** 563–572

Perez-Prat E, Narashimhan ML, Binzel ML, Botella MA, Chen Z, Valpuesta V, Bressan RA, Hasegawa PM (1992) Induction of a putative Ca^{2+}-ATPase mRNA in NaCl-adapted cells. Plant Physiol **100:** 1471–1478

Piao HL, Pih KT, Lim JH, Kang SG, Jin JB, Kim SH, Hwang I (1999) An Arabidopsis GSK3/shaggy-like gene that complements yeast salt stress-sensitive mutants is induced by NaCl and abscisic acid. Plant Physiol **119:** 1527–1534

Sanders D, Brownlee C, Harper JF (1999) Communicating with calcium. Plant Cell **11:** 691–706

Serrano R, Mulet JM, Rios G, Marquez JA, de Larrinoa IF, Leube MP, Mendizabal I, Pascual-Ahuir A, Proft M, Ros R, Montesinos C (1999) A glimpse of the mechanisms of ion homeostasis during salt stress. J Exp Bot **50:** 1023–1036

Sidler M, Hassa P, Hasan S, Ringli C, Dudler R (1998) Involvement of an ABC transporter in a developmental pathway regulating hypocotyl cell elongation in the light. Plant Cell **10:** 1623–1636

Snedden WA, Fromm H (1998) Calmodulin, calmodulin-related proteins and plant responses to the environment. Trends Plant Sci **3:** 299–304

Sze H, Liang F, Hwang I, Curran AC, Harper JF (2000) Diversity and regulation of plant Ca^{2+} pumps: insights from expression in yeast. Annu Rev Plant Physiol Plant Mol Biol **51:** 433–462

Trewavas AJ, Malho R (1998) Ca^{2+} signaling in plant cells: the big network! Curr Opin Plant Biol **1:** 428–433

Vitale A, Raikhel N (1999) What do proteins need to reach different vacuoles? Trends Plant Sci **4:** 149–155

Ward J, Reinders A, Hsu H, Sze H (1992) Dissociation and reassembly of the vacuolar H^+-ATPase complex from oat roots. Plant Physiol **99:** 161–169

Wimmers LE, Ewing NN, Bennett AB (1992) Higher plant Ca^{2+}-ATPase: primary structure and regulation of mRNA abundance by salt. Proc Natl Acad Sci USA **89:** 9205–9209

Wu S-J, Ding L, Zhu J-K (1996) SOS1, a genetic locus essential for salt tolerance and potassium acquisition. Plant Cell **8:** 617–627

Zhu JK, Liu J, Xiong L (1998) Genetic analysis of salt tolerance in Arabidopsis: evidence for a critical role of potassium nutrition. Plant Cell **10:** 1181–1191